ISSN 2229-5518

Modeling and Analysis Magnetic Field Shielding for Underground Power Cables

Suad Ibrahim Shahl

Abstract— This paper presents finite element model that can be used to investigate the effect of various shield geometries and shield materials around the 132KV Cross Linked Polyethylene (XLPE) single underground cable. In this paper, a three-dimensional eddy-current field model for calculating the eddy-current losses in the shielding model is proposed. The power loss density generated by eddy currents and the temperature rise due to the generated heat in the shielding model, must be analyzed as a coupled model using finite-element method when solving the governing thermal equations. The shielding effectiveness and the power losses are compared for shields with the same geometry but two shielding materials: conductive material (Aluminum) and magnetic material (Cold Rolled Steel). It is concluded that a partial ring shield is the optimal design for shielding the zone around the cable; also the losses in the Aluminum shield and the corresponding temperature rises are much lower when comparing with magnetic material shield.

Index Terms— Finite Element Method (FEM), Coupled Field Analysis, Shielding, Underground Cable

1 INTRODUCTION

Electromagnetic shielding is defined as the practice of reducing the electromagnetic field in a space by blocking the field with barriers made of conductive or magnetic materials. Shielding is typically applied to enclosures to isolate electrical devices from the 'outside world', and to cables to isolate wires from the environment through which the cable runs. The shielding can reduce the coupling of radio waves, electromagnetic fields and electrostatic fields. A conductive enclosure used to block electrostatic fields is also known as a Faraday cage. For static or slowly varying magnetic fields (below about 100 kHz) the Faraday shielding is ineffective. In these cases shields made of high magnetic permeability metal alloys can be used, such as sheets of Perm alloy and Mu-Metal. These materials don't block the magnetic field, as with electric shielding, but rather draw the field into themselves, providing a path for the magnetic field lines around the shielded volume. Since these materials have a reluctance much less than air, magnetic field lines can effectively be rerouted by providing an alternative path through a magnetic material. The amount of reduction depends very much upon the material used, its thickness, the size of the shielded volume and the frequency of the fields of interest and the size, shape and orientation of apertures in a shield to an incident electromagnetic field.

Shielding of power frequency magnetic fields from power lines by using metal plates is difficult because of the lack of support for metal settings. In the case of underground cables, the shielding option exists, as the soil provides a natural support for arrangements of metal plates. To reduce the magnetic field produced by the underground cables, a lot of shield structures and configurations can be used in the magnetic shielding for underground cables such as open and closed shield configurations. According to [1], it can be concluded that U- shield configuration can have good shielding performance when comparing with horizontal plate. Furthermore, in [2], a much better shielding efficiency is found for closed shields than for open shield configurations.

Transmission lines and underground cable magnetic fields can be calculated with analytic or numerical methods. When more complex structures need to be calculated, numerical calculations methods are useful. Numerical methods are needed, when the shielding effectiveness (SE) with different materials is studied [3]. A good shielding design should consider not only shielding efficiency but also power losses in the shield as well as shield cost, so this paper investigates shielding performance and electromagnetic losses in magnetic shielding for underground cables. The finite element method (FEM) is used to calculate eddy current losses in shielding. To predicate the temperature rises for the shielding, we employ the coupled solving electromagnetic-thermal scheme which calculates joule heat by ANSYS/EMAG is imported into ANSYS/THERMAL to analyze the temperature variation. Four shielding configurations are suggested to illustrate the effect of material property of shield as well as its geometrical shape and location with respect to the cable.

- *Dr. Suad Ibrahim Shahl is Assist. Professor in Electrical Engineering Department in University of Technology, Iraq,. E-mail: 30053@uotechnology.edu.iq*

2 FORMULATION 3D FEM

2.1 Governing Equations

Time harmonic electromagnetic field which is governed by Maxwell's equation with displacement current neglected, quasi static Maxwell's approximation as

$$\nabla \times \vec{H} = \vec{J} \quad (1)$$

$$\nabla \times \vec{E} = (\partial \vec{B})/\partial t \quad (2)$$

$$\nabla \cdot \vec{B} = 0 \quad (3)$$

From (3), magnetic vector potential $\vec{A}$ is

$$\vec{B} = \nabla \times \vec{A} = \mu\vec{H} \quad (4)$$

Using Maxwell's equation in which the magnetic vector potential and the electric scalar potential are introduced, the 3D eddy current field equations can be written as [4], [5]

$$\nabla \times 1/\mu \, \nabla \times \vec{A} = \vec{J}_{total} = \vec{J}_s + \vec{J}_e = -\sigma\nabla\emptyset - j\omega\sigma\vec{A} \quad (5)$$

Where J_{total} is the total current density, J_s is the source current density; J_e is the eddy current density and ∅ is electric scalar potential.

Power loss is generated at the conductor regions due to the induced eddy current. The heat source due to power loss increases the temperature of the shields region. Heating loss calculated by the magnetic field analysis, is used as the input data to predict the temperature rise for the thermal analysis.

The coupled electromagnetic-thermal constitutive equations [6] are:

$$\{q\} = [\Pi]\{J\} - [K]\{\nabla T\} \quad (6)$$

$$\{J\} = [\sigma](\{E\} - [\alpha]\{\nabla T\}) \quad (7)$$

Substituting [Π] with T[α] to further demonstrate the coupling between the above two equations

$$\{q\} = T[\alpha]\{J\} - [K]\{\nabla T\} \quad (8)$$

where:
[Π] is Peltier coefficient matrix ([Π] = T[α]), T = absolute temperature, q = heat flux vector (output as TF), J is electric current density, K is thermal conductivity, ∇T is thermal gradient (output as TG), σ is electrical conductivity and E is electric field.

2.2 Shielding Model

A 132KV XLPE single cable is considered to be investigated in this work, which is buried about the 1-meter under the surface ground. For purpose of creating the finite element model the real geometry of the cable was simplified and presented as a combination of co-axial cylinders, the phase conductor at the center of the cable with sector length of 500mm, and then comes a semiconducting conductor shield, the insulation, semiconducting insulation shield, shield, and finally covering jacket.

In this work, four magnetic shield configurations are proposed. These configurations are shown in Fig.1 and have different angle of curvature (90°, 180°, 270°, 360°) that is placed around the cable along the horizontal axis. For the reason of cost-effectiveness the thin metal shields with the thickness of 20mm at 50mm from the underground cable is used.

The material selected to create the magnetic shield has been conductive material (aluminum) and ferromagnetic material (cold rolled steel). Their main parameters are shown inTable1, which includes the coefficients needed in modeling. The shielding efficiency of magnetic fields in the quasi static systems it is defined in decibels (dB) as:

$$SE = 20\log 10\left[\frac{B_0(x,y,z)}{B_{Shielded}\ (x,y,z)}\right] \quad (9)$$

Where B_o is the magnetic field in the absence of the shield, and $B_{shielded}$ is the magnetic field after placing the shield.

The magnetic shielding efficiency is very dependent on the skin depth δ based on the assumption of a quasi-steady state, with a constant frequency, and with the electric and magnetic conductivities of the materials under consideration remaining constant.

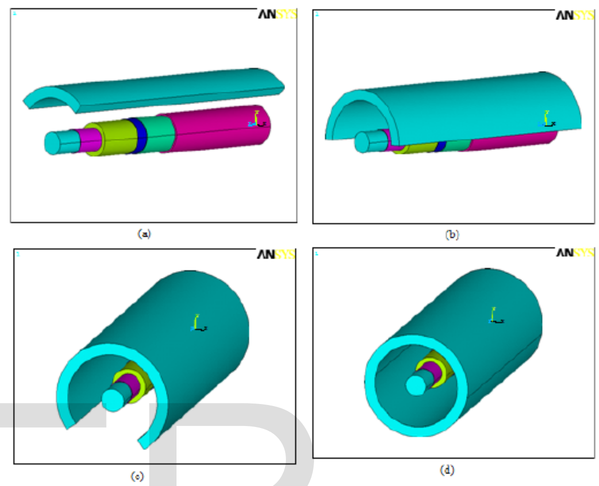

Fig.1.Shielding design with different angle of curvature (a) 90°, (b) 180°, (c) 270°, (d) 360°

TABLE 1
PARAMETERS FOR THE SHIELD MATERIALS

Material	μ	σ (S/m)	δ(cm) at 50Hz	Thermal conductivity (W/m.^{0}C)	Convection coefficient (W/m^2.k)
Aluminum	1	$35*10^6$	1.2	205	25
cold rolled steel	200*	$6.3*10^6$	0.2	51.9	5

* In all the simulations a linear properties was assumed

3 RESULTS AND DISCUSSION

The numerical simulation of the model is carried out with ANSYS 14.0 The results were calculated under worst summer conditions with the maximum current carrying in cable combined with the high moisture content. The current rating for the copper conductor is selected of 20KA; ambient temperature and soil temperature assume 70°C.

Fig.2 shows a comparison of the shielding efficiency, for four shield configurations and two materials.

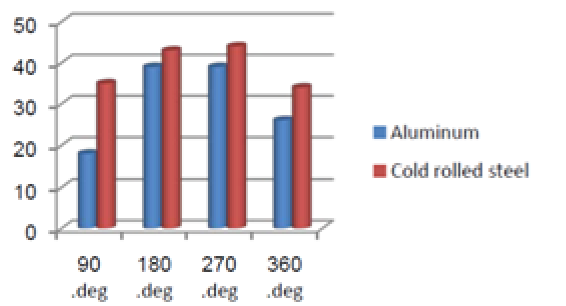

Fig.2. Average of the shielding effectiveness (SE) for the magnetic field in decibels (dB) along the focal points on height 0.5m

It is observed that the magnetic shielding efficiency is best for Cold rolled steel, but it is not bad for Aluminum. Additionally, the results indicate that the maximum shielding effectiveness is achieved with the semi-cylinder of the shield (bending angle of 180^0 and 270^0). So increasing angle of curvature of the shield gives a better shielding efficiency because the cable position is closer to the shield.

Concerning the losses, the shielding material aluminum with the each geometry is better in lower power losses than for cold rolled steel as shown in Fig.3.

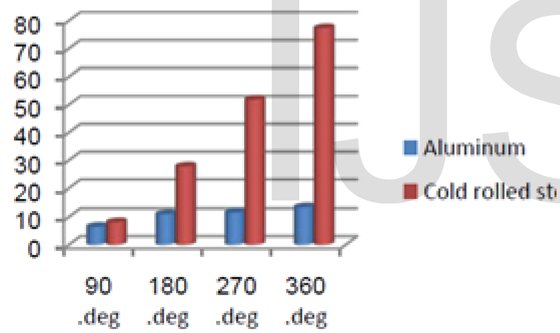

Fig.3. Power losses, P_{Loss} (Watt) in shield

When comparing four shield configurations, the increasing angle of curvature of the shield causes approximately double losses in the Cold rolled steel shields. This gives rise to a higher average temperature of the shield material. The Aluminum shield is preferred when low loss is important and the corresponding average temperature rises is much lower. A sample of these results is illustrated in post-processing in ANSYS/FLOTRAN depicts Figs. (4-7).

For case aluminum shield material the average values of temperature gradient are low and the maximum temperature gradient occurs at edge of model shield toward the axis of the middle model, with increase bending angle as shown in Fig.8.

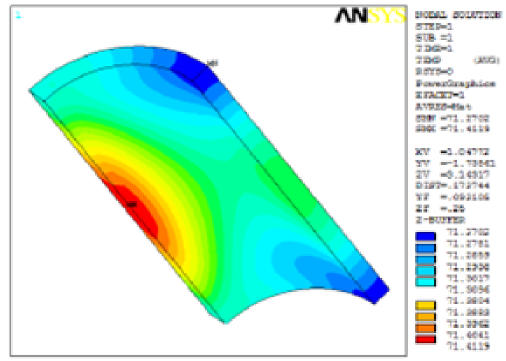

(a) The temperature distribution

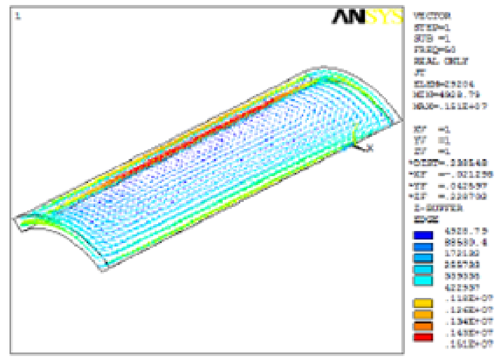

(b) Eddy current distribution (real solution)

Fig.4. Post-processing in ANSYS/FLOTRAN for shield material Aluminum and 90^o angle of curvature

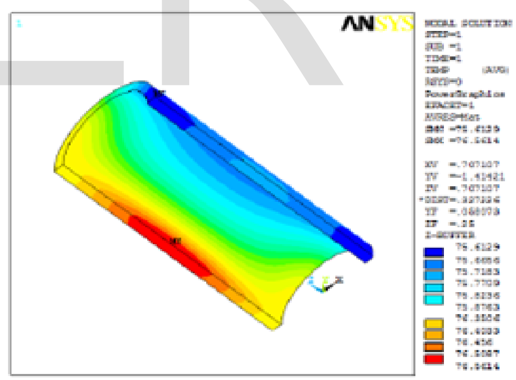

(a) The temperature distribution

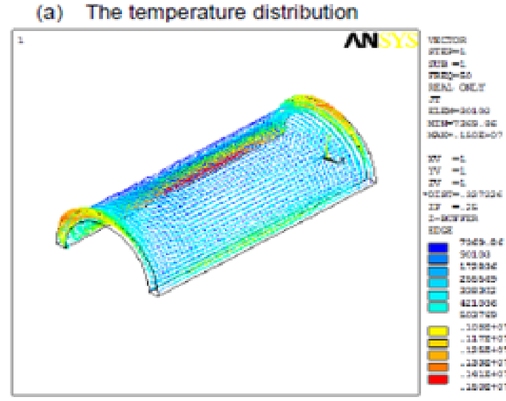

(b) Eddy current distribution (real solution)

Fig.5. Post-processing in ANSYS/FLOTRAN for shield material Aluminum and 180^o angle of curvature

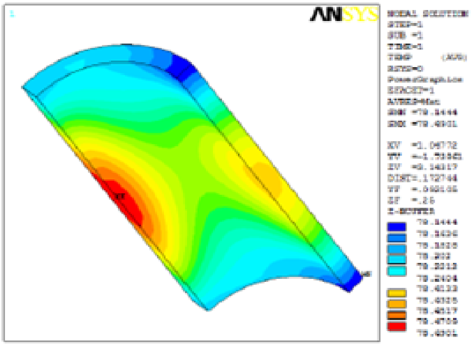

(a) The temperature distribution

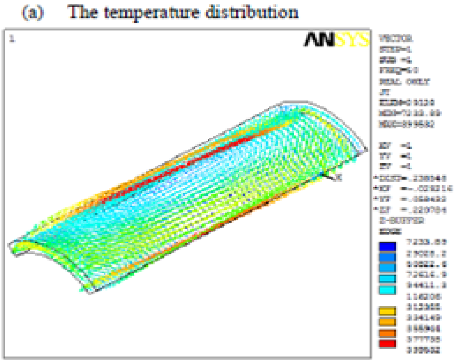

(b) Eddy current distribution (real solution)

Fig.6. Post-processing in ANSYS/FLOTRAN for shield material Cold rolled steel and 90° angle of curvature.

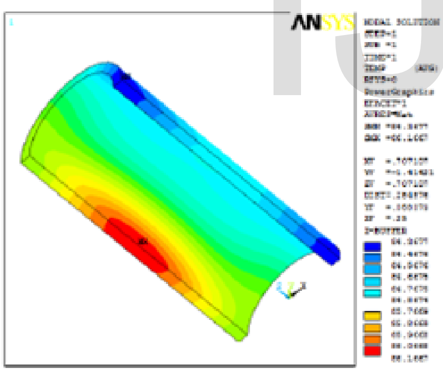

(a) The temperature distribution

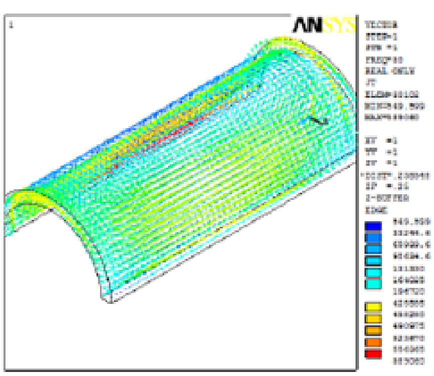

(b) Eddy current distribution (real solution)

Fig.7. Post-processing in ANSYS/FLOTRAN for shield material Cold rolled steel and 180° angle of curvature.

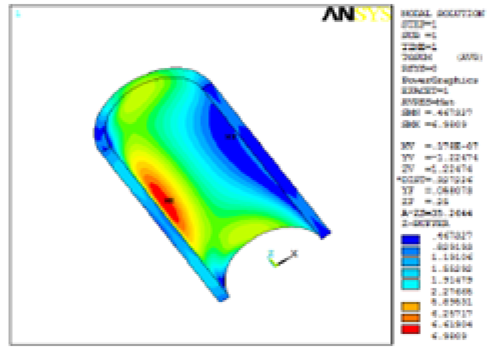

(a)

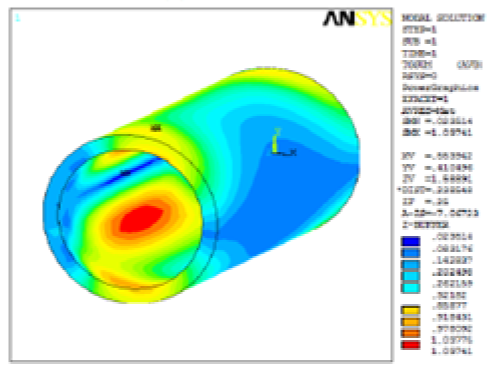

(b)

Fig.8. Temperature gradient, TG (°C/m) in the aluminum shield material with bending angle (a) 180° and (b) 360°

Fig.9. presents the average values of temperature gradient for case cold rolled steel shield material. It can be seen that of temperature gradient increase rapidly with the increase of the bending angle.

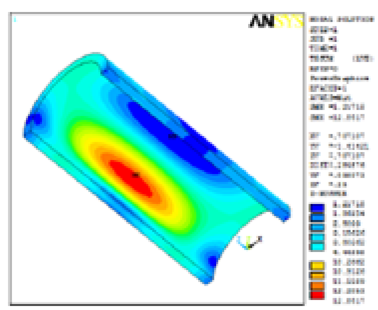

(a)

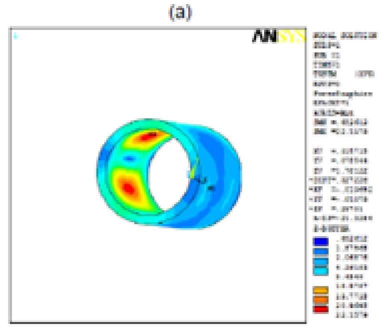

(b)

Fig.9. Temperature gradient, TG (°C/m) in the cold rolled steel shield material with bending angle (a) 180° and (b) 360°

Table 2 shows a comparison of the average temperature rises in all configurations.

TABLE 2
COMPARISON OF SHIELD CONFIGURATION ON AVERAGE TEMPERATURE, T_{AVE}(^{O}C) IN SHIELD

Angle of curvature / Material	90°	180°	270°	360°
Aluminum	71.341	76.087	70.859	70.786
cold rolled steel	78.317	85.268	89.174	92.705

The magnitude of heat generation in the shielding model is determined as Heat flux density, TF (watt/m^2). In the case of Aluminum shield material there is fluctuate in the magnitude density of heat flux according to the bending angle as shown in Fig. 10. Additionally, Fig.10 also demonstrates that the bending angle at which the shield acts as the best director of flux above the shield. Sequentially, it can be observed from Fig. 11 that Cold rolled steel has about 3 times more loss than Aluminum. Fig. 11 also demonstrates that the increasing angle of curvature of the shield is an affected on heat flux density.

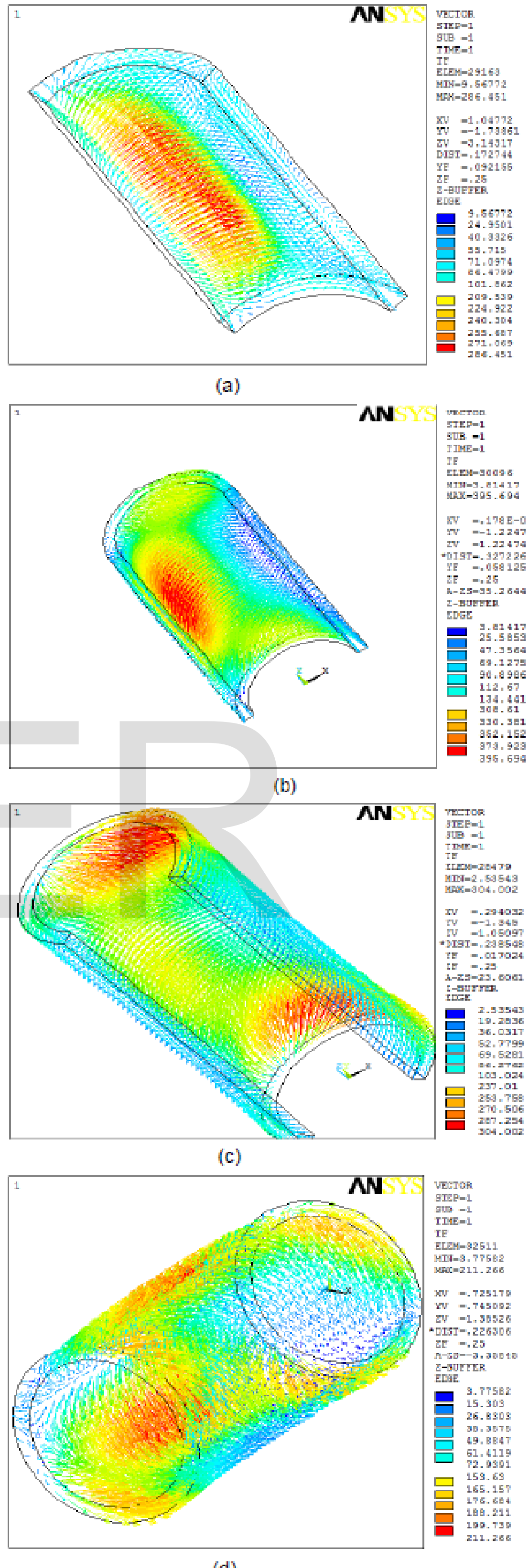

Fig.10. Heat flux density, TF (watt/m^2) in the aluminum shield material with bending angle (a) 90^{o}, (b) 180^{o}, (c) 270^{o} and (d) 360^{o}

ISSN 2229-5518

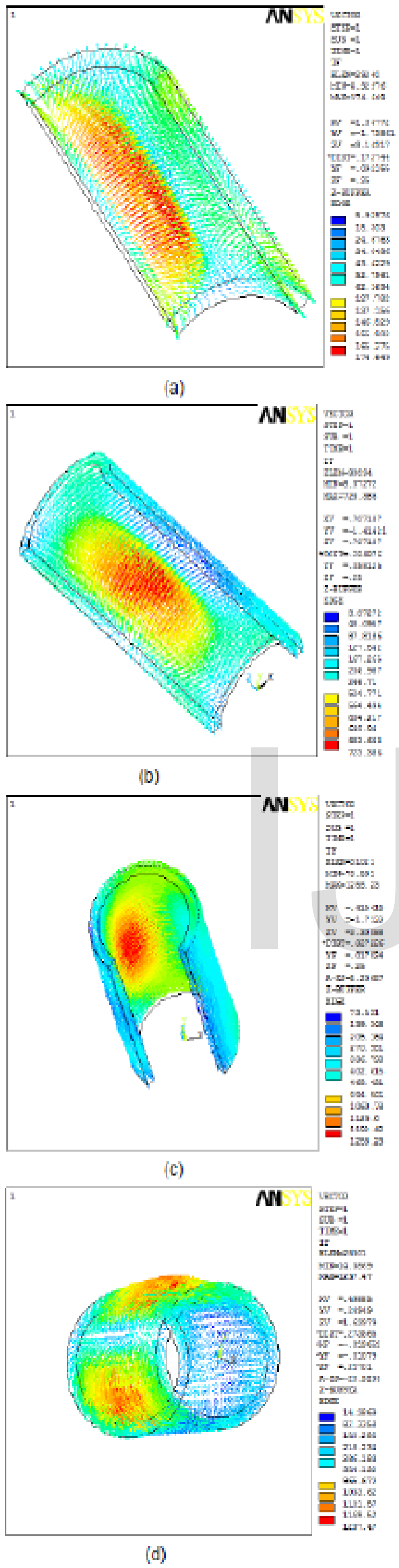

Fig.11. Heat flux density, TF (watt/m^2) in the cold rolled steel shield material with bending angle (a) 90^0, (b) 180^0, (c) 270^0 and (d) 360^0

4 CONCLUSION

The FEM solution of 132kV underground cable and magnetic shield designs has been presented. This work is also presented to determine the parameters required to optimize the shield design. The results indicate that a high shield material permeability with high bending angle for shielding around cable present high shielding efficiency. While the losses in the Aluminum shield and the corresponding temperature rises are much lower when comparing with magnetic material shield, but for reasons of cost prefers magnetic shield material.

REFERENCES

[1] Juan C. del Pino-Lopez and Pedro Cruz-Romero, *Magnetic field shielding of underground cable duct banks*, Progress In Electromagnetics Research, Vol. 138, 1-19, 2013.

[2] J.R. Riba Ruiz and X. Alabern Morera, *Magnetic shields for underground power lines*, International Conference on Renewable Energy and Power Quality (ICREPQ' 04), 2004.

[3] P. Sergeant and S. Koroglu, *Electromagnetic losses in magnetic shields for buried high voltage cables*, Progress In Electromagnetics Research, Vol. 115, 441- 460, 2011.

[4] J. Weiss and Z. Csendes, "A one-step finite element method for Multiconductor skin effect problems," *IEEE Trans. Power App. Sysr.*, vol. PAS-101, no. 10, pp. 3796-3803, Oct. 1982.

[5] H.K. Kim, et al., " Efficient Technique for 3-D Finite Element Analysis of Skin Effect in Current-Carrying Conductors", IEEE Trans. on Magnetics, Vol. 40, No. 2, pp.1326-1329, March 2004.

[6] L.D. Landau and E.M. Lifshitz. "Electrodynamics of Continuous Media". Course of Theoretical Physics. Vol. 8. 2nd Edition. Butterworth-Heinemann. Oxford. 1984.